

# CFD Simulation and Measurement of Flow Forces Acting on a Spool Valve

**Ing. Patrik Bordovsky**

RWTH Aachen University, Institute for Fluid Power Drives and Controls (IFAS), Aachen, Germany, E-Mail: Patrik.Bordovsky@ifas.rwth-aachen.de

**Dr.-Ing. Katharina Schmitz**

Walter Hunger International GmbH, Würzburg, Germany, E-Mail: K.Schmitz@hunger-international.de

**Professor Dr.-Ing. Hubertus Murrenhoff**

RWTH Aachen University, Institute for Fluid Power Drives and Controls (IFAS), Aachen, Germany

## Abstract

Directional control valves are widely used in hydraulic systems to control the flow direction and the flow rate. In order to design an actuator for such a valve a preliminary analysis of forces acting on the spool is necessary. The dominant axial force is the so called steady flow force, which is analysed within this study. For this purpose a 2/2-way spool valve with a sharp control edge was manufactured and investigated. CFD simulations were carried out to visualize the fluid flow inside the valve. The measured and simulated axial forces and pressure drops across the test valve are compared and show good qualitative correlation. However, the simulated values of axial forces are in average by 32 % lower compared with the measured ones. Therefore, the components of the axial force were scrutinized revealing a dominance of the pressure force acting on ring areas in the spool chamber. Although CFD simulations are preferably used to save resources, the results of this study emphasise the importance of the experiments.

**KEYWORDS:** CFD simulation, Flow force, Spool valve, Validation

## 1. Introduction

One of the challenges when designing actuators for directional spool valves is the estimation of flow forces acting on spools. Especially when developing proportional or servo-valves the flow forces play an important role as they have a significant impact on dynamic performance and linearity of the valves. It is generally desired to reduce the flow forces both to improve the static and dynamic behavior of the valves and to reduce

the required power consumption of the actuators. For this purpose much research has been conducted already.

The first experimental and theoretical studies focused mainly on predicting and describing the flow forces acting on spool valves with sharp control edges. In the last decades, CFD (Computational Fluid Dynamics) simulations were performed in order to analyse and/or reduce the flow forces. For example, Lisowski /1/ validated a three dimensional CFD simulation of a directional control valve and proposed a solution for reducing flow forces. Yaun /2/ investigated the flow forces experimentally and using CFD simulations and provided recommendations for CFD simulations. Concerning the turbulence, different models were proposed by Schuster /3/ in favour of the k- $\epsilon$  model and by Tanaka /4/ in favour of the SST model.

Within this paper the simulated and measured steady flow force acting on a test valve spool are compared to each other. First, the relevant theory is described. Second, the test valve and the test rig are introduced. The third part is dedicated to the setting of CFD simulations and the simulation and experiment results are shown and discussed in the last part of this paper.

## 2. Flow Forces

In order to stroke a spool valve, an actuator must exert the force  $F_a$  (Figure 1).

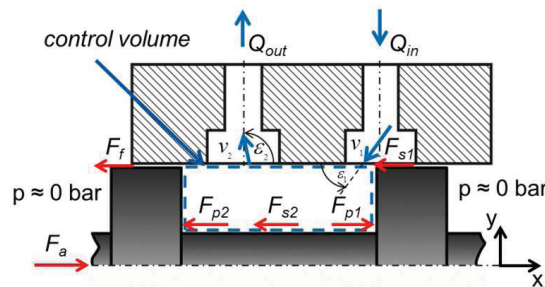


**Figure 1:** Forces acting on a spool

Assuming only axial forces, the spool movement can be described using the equation of motion (1).

$$m\ddot{x} = \sum F = F_a + F_{p1} - F_{p2} - F_f - F_{s1} - F_{s2} \quad (1)$$

The friction force  $F_f$  is a result of dry and skin friction in the gap between the spool and sleeve. The shear forces  $F_{s1}$  and  $F_{s2}$  are axial components of a drag, which is caused by fluid motion across the surface of the spool. Applying Bernoulli's law, the pressure forces  $F_{p1}$  and  $F_{p2}$  acting on both ring areas of spool can be summed up.

The sum of forces  $F_{s2}$ ,  $F_{p1}$  and  $F_{p2}$  equals the so called flow force. It results from fluid flowing through the valve orifices and in the valve chamber. The analytical description of flow forces can be derived using the law of conservation of momentum /5/, which says that the rate of change of momentum of a system equals the sum of all forces acting on the system.

All forces apart from flow forces and the radial clearance between the spool and the sleeve are usually neglected. Assuming an incompressible fluid and control volume defined by the geometric boundaries of the valve chamber (Figure 1), the flow force  $F_{fl}$  is described by equation (2).

$$\rho L \frac{\partial Q}{\partial t} - \rho Q v_1 \cos \varepsilon_1 - \rho Q v_2 \cos \varepsilon_2 = -F_{fl} \quad (2)$$

The first term of equation (2) describes the unsteady flow force and is not considered in this study. The steady flow force  $F_{fl,s}$  is composed of the second and the third term of equation (2). The second term describes the inflow momentum and the third term the outflow momentum, which is usually being neglected. This leads to a common definition of the steady flow force (3).

$$F_{fl,s} = \rho Q v_1 \cos \varepsilon_1 \quad (3)$$

However, different formulas describing the inflow velocity  $v_1$  have been derived as published in /6/. Combining equation (3) with the orifice equation (4)

$$Q = \alpha_D \pi dx \sqrt{\frac{2\Delta p}{\rho}} \quad (4)$$

and equation (5) describing the definition of the inflow velocity /5/,

$$v_1 = \frac{Q}{\sin \varepsilon_1 \pi dx} \quad (5)$$

the steady flow force  $F_{fl,s}$  can be expressed by equation (6) /5/.

$$F_{fl,s} = 2 \alpha_D^2 \pi dx \Delta p \frac{\cos \varepsilon_1}{\sin \varepsilon_1} \quad (6)$$

### 3. Experimental Setup

For the purpose of investigating steady flow forces a 2/2-way proportional test spool valve was manufactured at the Institute for Fluid Power Drives and Controls (IFAS) of RWTH Aachen University.

#### 3.1. Test Valve

**Figure 2** shows cross sections of the test valve, which is composed of a valve block, sleeve, spool and two lids. The test valve has two main ports P and T and two leakage ports L. Both the spool and the sleeve are removable. Hence, it is possible to replace them and investigate the influence of different shapes of control edges on flow forces.

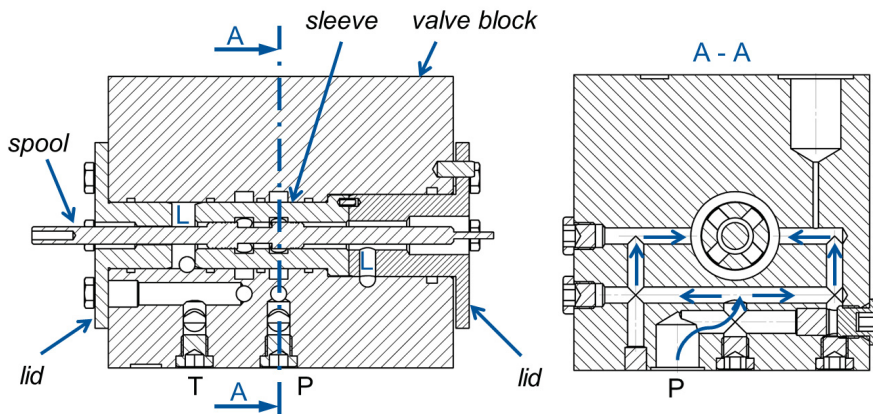


**Figure 2:** Longitudinal (left) and lateral (right) cross section of the test valve

On the left hand-side of the spool, a connection to the load cell is provided, whereas a displacement sensor is connected to the right-hand side of the spool. In order to simplify CFD simulations, symmetrical in- and outflow ports to, resp. from the spool were designed (see Figure 2).

A preliminary survey of directional proportional valves from different manufacturers was carried out to match the dimensions of the test valve with dimensions of common valves. It was found out, that the ratio between the shank and the spool diameter is about 0.6. The diameter of the ports in the sleeve usually equals the shank diameter. Relevant dimensions of the valve are presented in Table 1. The nominal flow rate of the test valve is approximately 109 l/min, at the pressure drop of 35 bar and maximum stroke of 1 mm. The nominal flow rate was measured with the hydraulic oil HLP46 at 60 °C.

| Dimension        | Value | Unit          |
|------------------|-------|---------------|
| Shank diameter   | 6     | mm            |
| Spool diameter   | 10    | mm            |
| Chamber length   | 20    | mm            |
| Radial clearance | 8     | $\mu\text{m}$ |

**Table 1:** Dimensions of the test valve

In order to eliminate friction forces, circumferential grooves were manufactured on the spool as illustrated in **Figure 3**.



**Figure 3:** Test valve spool

### 3.2. Measurement

IFAS features a test rig designated for measurements of characteristics of industrial valves. For the purpose of measurement of flow forces the test rig was modified (**Figure 4**).

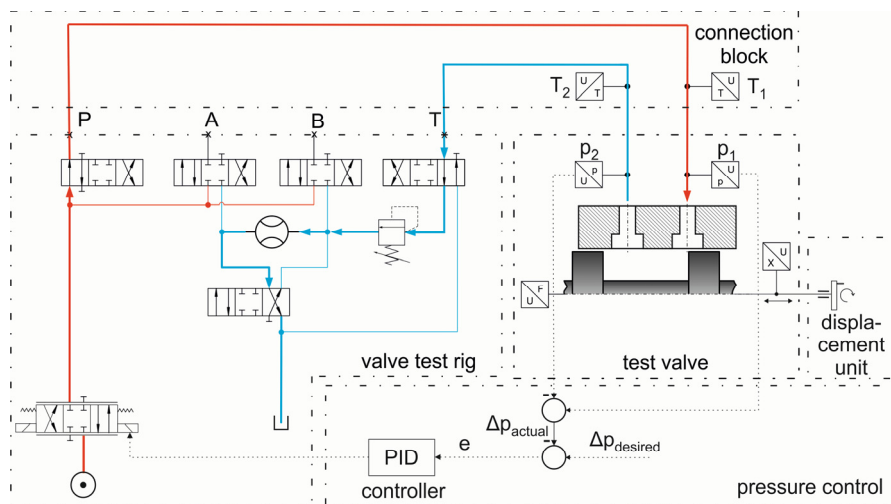


**Figure 4:** Circuit diagram of the test rig

The hydraulic power unit supplies the circuit with constant pressure. The switching valves are used to control the fluid flow from the hydraulic power unit through the test valve to a tank. The pressure relief valve was used to keep the pressure  $p_2$  at 100 bar in order to avoid cavitation. The test valve is mounted on the connection block using the interface for industrial valves of the nominal size 16. The servo-valve controls the

pressure drop over the test valve. The stroke of the test valve is set manually with the displacement unit. The main part of the test rig is shown in **Figure 5**.

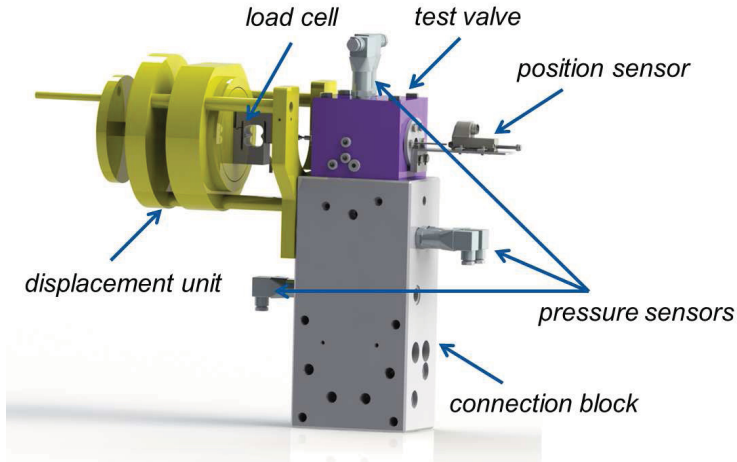


**Figure 5:** Main part of the test rig

### 3.2.1. Measurement of Flow Forces

The oil temperature of 40 °C in the tank was controlled and the oil temperature in the test valve reached between 55 and 60 °C depending on the actual operating point.

Since only the steady flow force  $F_{fl,s}$  was investigated, measurements in discrete operation points were carried out. However, it is not possible to measure directly the steady flow force. Instead, the axial force  $F_{ax}$  (7) was measured, considering that the friction force  $F_f$  acts against the direction of the steady flow force.

$$F_{ax} = F_{fl,s} + F_{s1} - F_f \quad (7)$$

The axial forces were measured at 10 different valve strokes beginning with 0.1 mm and ending at 1 mm. At each stroke, the pressure drop was set and controlled by the servo-valve.

### 3.2.2. Measurement of Friction Forces

The friction force cannot be measured separately during the fluid flow. Hence, the friction force was measured when the port T (Figure 4) was closed. So the spool chamber was pressurized and the spool was moved as slowly as possible. As shown in **Figure 6**, the friction forces are almost negligibly dependent on the spool stroke and on the chamber pressure.

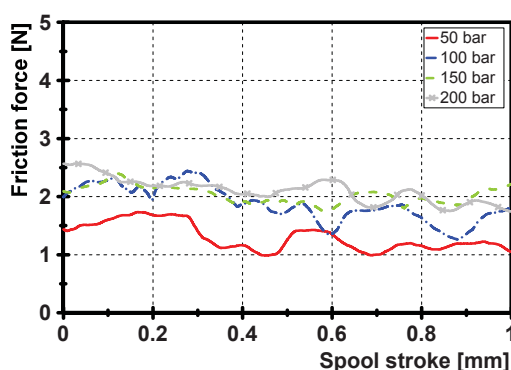


**Figure 6:** Friction forces at different pressure levels

## 4. CFD Simulation

The CFD simulations were carried out using ANSYS CFX 16.0 within ANSYS Workbench assuming symmetrical three dimensional steady incompressible isothermal viscous fluid flow. In addition, both the radial clearance and the friction between the spool and the sleeve were neglected.

### 4.1. Flow Domain

The full flow domain is shown in **Figure 7**. Thanks to the symmetry of the flow domain only a quarter model was used for the simulations. Hence two sym-metry planes were defined. All walls were considered as hydraulically smooth.

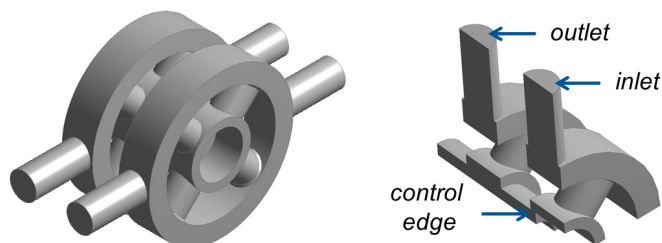


**Figure 7:** Full (left) and quarter (right) model of the fluid domain

## 4.2. Mesh

The meshes were created in ANSYS Meshing. The fluid domain was meshed with tetrahedral and prism elements with the average mesh count about 1,2e6 nodes (3,5e6 elements). The boundary layers were resolved with 10 prism layers as shown in **Figure 8**. The height of the first prism layer was set to 5  $\mu\text{m}$ . In order to achieve high quality meshes, local sizing functions were used. So the mesh metric “Skewness” was below 0.8 and the mesh metric “Orthogonal Quality” was above 0.2 meaning a good mesh quality according to [7].

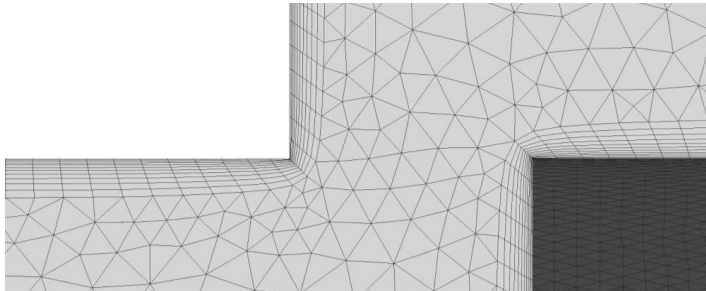


**Figure 8:** Detailed view on the mesh in the region of the sharp control edge

## 4.3. Simulation Parameters

The parameters of CFD were set according to recommendations described in [7] to achieve as accurate results as possible. Furthermore, a sensitivity study of different parameter sets has been carried out including different boundary conditions, turbulence models and their parameters, timescale control, advection scheme etc. Especially the choice of the turbulence model and the near wall treatment can have a significant impact on the accuracy of simulation results.

Based on the sensitivity study, the RNG  $k\text{-}\epsilon$  model and the scalable wall function were chosen. At the inlet, the mean flow velocity calculated from the measurement data was defined. The reference pressure was set to 100 bar, so the average static pressure of 0 bar was set at the outlet. The RMS (root mean square) residuals of  $1\text{e-}5$  were used as the convergence criteria. Additionally, the axial force acting on the spool and the inlet pressure were defined as target variables. Other parameters which are not discussed in this paper were left as default. All simulations were performed considering the hydraulic oil HLP46 with constant density of  $856\text{ kg/m}^3$  and constant kinematic viscosity of  $24\text{ mm}^2/\text{s}$ .



## 5. Results

The results of the simulations and a comparison with the measurements are presented in this chapter. Figures 9 – 12 depict the results of the CFD simulation carried out for the pool stroke of 1 mm at pressure drop of 50 bar.

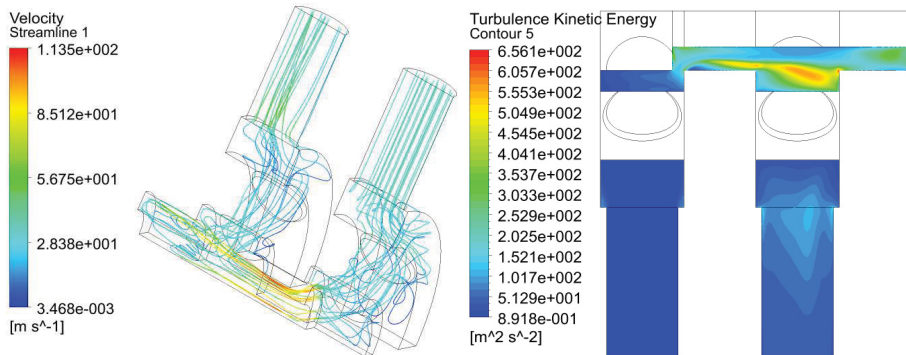


**Figure 9:** Streamlines (left) and turbulent kinetic energy (right) across the flow domain

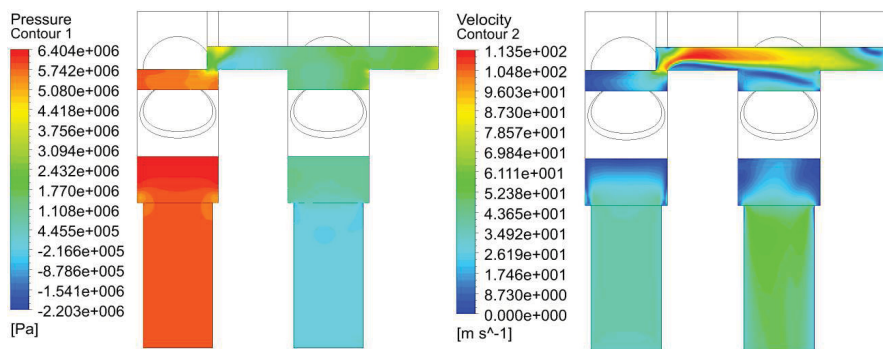


**Figure 10:** Static pressure (left) and velocity (right) across the symmetry plane

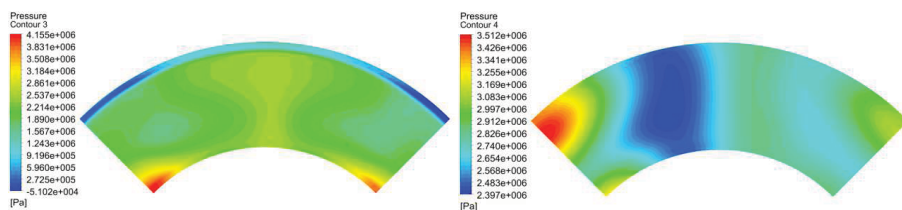


**Figure 11:** Static pressure on the ring area near the control edge (left) and on the opposite land ring area (right)

**Figure 9** demonstrates the turbulent character of the flow with strong curvatures and flow separations. The static pressure and the velocity across the symmetry plane are depicted in **Figure 10**. The pressure distribution on the ring area opposite the control edge is unsymmetrical as shown in **Figure 11**. Further-more, two recirculation zones in the spool chamber are visible in **Figure 12**.

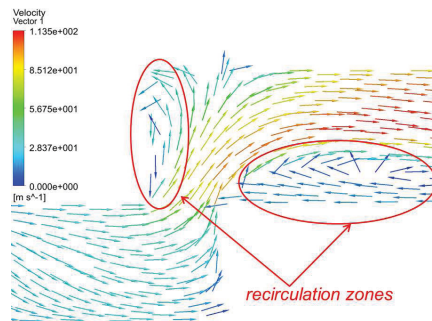


**Figure 12:** Velocity vectors in the vicinity of the control edge

The overview of the components of the simulated axial force is depicted in **Figure 13**.

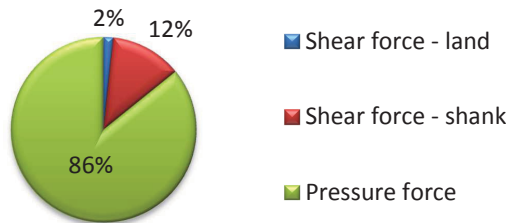


**Figure 13:** Simulated components of axial force

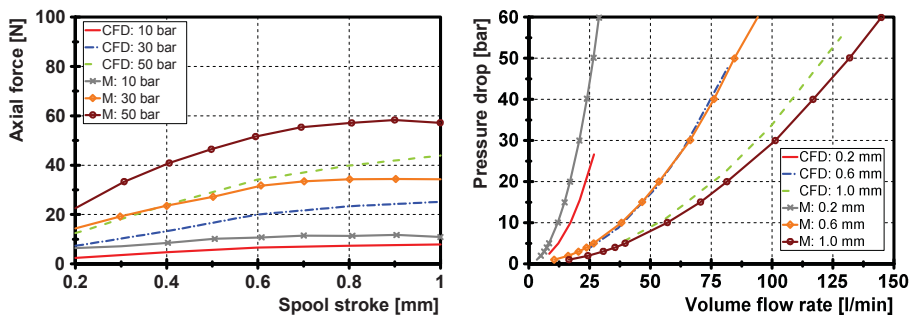


**Figure 14:** Measured and simulated axial forces (left) and pressure drops (right)

Since the mean flow velocity defined in the simulation was obtained from the measurement data, the measured and the simulated axial forces and inlet pressures are compared to each other (see **Figure 14**).

## 6. Discussion and Conclusions

The measured and simulated axial forces and pressure drops coincide qualitatively. However, the simulated values of axial forces are in average by 32 % lower compared with the measured ones. This highlights the importance of experiments, as the CFD simulations can be error prone. Since a very good reproducibility of the measurements has been achieved it is assumed, that the accuracy of the measurements is very high. Only the measured friction forces are likely affected by poor sensor accuracy in the lower measurement range. Moreover, it was assumed that the measured friction force corresponds to the friction force, which acts on the spool, while the fluid is flowing. Although all recommendations /7/ for increasing the accuracy of CFD simulations were fulfilled, the simulation results are inaccurate. It was observed for one particular case, that the pressure force entails 86 % of the simulated axial force. So the potential source of uncertainty is the pressure distribution in the spool chamber and especially on the ring areas of the spool.

Further investigations including transient simulations will be undertaken to increase the accuracy of the CFD simulations and to optimize existing formulas for the estimation of flow forces.

## 7. References

- /1/ Lisowski, E. "Three dimensional CFD analysis and experimental test of flow force acting on the spool of solenoid operated directional control valve", *Energy Conversion and Management*. 2013.
- /2/ Yuan, Q. "Flow Forces Investigation through Computational Fluid Dynamics and Experimental Study", *Proceedings of the 9th International Fluid Power Conference*. Aachen. Germany. 2014.
- /3/ Schuster, G. *CFD-gestützte Maßnahme zur Reduktion von Strömungskraft und Kavitation am Beispiel eines hydraulischen Schaltventils*. PhD thesis. Shaker Verlag, Aachen. 2005.
- /4/ Tanaka, K. "Steady and Unsteady Flow Force acting on a Spool Valve". *Conference Proceedings of Power Transmission and Motion Control*. Bath. United Kingdom. 2012.
- /5/ Murrenhoff, H. *Grundlagen der Fluidtechnik - Teil 1: Hydraulik*. Shaker Verlag, Aachen. 2012.

- /6/ Schrank, K. "Beschreibung der Strömungskraft in Längsschieber-ventilen mittels Impulserhaltung", *O+P Journal*. 2013.
- /7/ ANSYS Documentation (Version 16.0).

## 8. Nomenclature

|                               |                                      |                   |
|-------------------------------|--------------------------------------|-------------------|
| $d$                           | Spool diameter                       | m                 |
| $F_a/F_f$                     | Actuator/Friction force              | N                 |
| $F_{ax}$                      | Axial force acting on the spool      | N                 |
| $F_{fl}(F_{fl,s})$            | (Steady) Flow force                  | N                 |
| $F_{s1}/F_{s2}$               | Shear force on the spool land/shank  | N                 |
| $F_{p1}/F_{p2}$               | Pressure forces acting on ring areas | N                 |
| $L$                           | Length of the spool chamber          | m                 |
| $\Delta p$                    | Pressure drop across the valve       | Pa                |
| $Q_{in}/Q_{out}$              | Inflow/Outflow volume flow rate      | m <sup>3</sup> /s |
| $v_1/v_2$                     | Inflow/Outflow fluid velocity        | m/s               |
| $m$                           | Mass                                 | kg                |
| $x$                           | Spool stroke                         | m                 |
| $\alpha_D$                    | Discharge coefficient                | -                 |
| $\varepsilon_1/\varepsilon_2$ | Inflow/Outflow fluid jet angle       | °                 |
| $\rho$                        | Fluid density                        | kg/m <sup>3</sup> |